THE NATURE OF ATMOSPHERIC TURBULENCE EFFECTS ON IMAGING AND PSEUDO-IMAGING SYSTEMS, AND ITS QUANTIFICATION

David L. Fried

the Optical Sciences Company

P. O. Box 446, Placentia, CA 92670, USA

ABSTRACT

Over the last two decades, an extensive body of knowledge has been developed concerning the effects of atmospheric turbulence on optical propagation. Much of this is directly relevant to astronomical imaging, and with proper interpretation, to the type of pseudo-imagery that is of concern to us at this conference. This paper will provide an overview of this matter, hopefully with sufficient insight developed that the reader will be able to quickly estimate the nature and magnitude of the turbulence effects to be expected in a pseudo-imagery process. The paper starts with a review of turbulence effects on conventional imagery, reviewing the "nondimensional" nature of the turbulence statistics, presenting the local measure of the optical strength of turbulence, C_N^2, and developing the resolution scale, r_o It presents a statistical view of the nature of the wavefront distortion geometry, indicating the dominance of the random wavefront tilt component. The MTF for conventional imagery and for speckle interferometry (Labeyrie) is presented with comments concerning their relationship. Following that, the foundation of the speckle imagery concept (Knox-Thompson) is presented. Results are then set forth for the allowable spectral bandwidth in speckle techniques, as well as results defining the allowable field-of-view size (isoplanatism) and the allowable exposure time for speckle techniques. Taken all together, these results provide a basis for estimating most of the significant effects of atmospheric turbulence in speckle interferometry and speckle imagery.

https://doi.org/10.1017/S0252921100118639 Published online by Cambridge University Press

1. INTRODUCTION

The effects of atmospheric turbulence on large aperture and large baseline imaging and pseudo imaging systems is the underlying fact responsible for this meeting, and as such, needs no general explanatory comments here. However, the circumvention of these effects, which is our real concern here, calls for a sound and to some extent, quantitative understanding of the processes involved. It is the objective of this paper to provide just this type of understanding. As such we shall, for the most part, avoid analytic development, presenting only those bits that will provide a quick glimpse of what is involved, and generally shall simply present results and their interpretations. We shall be particularly interested in presenting results which lead to quantitative estimates of what is to be expected.

We shall start with a general description of the nature of atmospheric turbulence, of its optical effects, and of the measure of the optical strength of turbulence, C_N^2, and its distribution in the atmosphere. We shall then turn to an examination of the statistics of wavefront distortion, which will lead us to introduce the general wavefront distortion scale length, r_o. From this, we shall then be able to move on to a discussion of the shape of the distorted wavefront and a statistical description of these shapes, noting along the way the significant role played by tilt-like wavefront distortion.

With these results in hand, we will then move on to a presentation of the effect of turbulence on the optical transfer function of conventional imagery for long and for short exposures, and for a two aperture, (i.e., a Michelson stellar interferometer), imaging system. This will then lead naturally into our presentation of the Labeyrie speckle interferometry concept and an examination of the optical transfer function to be associated with that technique. In conjunction with this, we will also consider the Knox-Thompson algorithim, presenting an explanation of the underlaying principles.

https://doi.org/10.1017/S0252921100118639 Published online by Cambridge University Press

Consideration of these two speckle based pseudo imagery processes introduces the problem of estimating the useful spectral bandwidth, the allowable field-of-view, and the proper exposure time. We will provide an estimate of the first of these starting from wavefront distortion statistics. To treat the latter two matters we shall present some results developed for adaptive optics and indicate how they can be applied to the speckle based processes.

Throughout this presentation we shall try to provide the formulas necessary for a quantitative evaluation. Where possible, we shall present sample quantitative results.

2. ATMOSPHERIC TURBULENCE STATISTICS

Turbulence is basically a random irregularity in what is otherwise a smooth, uniform, large scale flow. The Navier-Stokes equation, which governs fluid flow, is nonlinear. As a consequence, the low spatial frequency components of a flow pattern, which are an almost unavoidable feature of the process that puts energy into the flow, will give rise to higher spatial frequency components, and these, inturn, give rise to yet higher spatial frequency components — and "so proceed ad infinitum", almost. In this manner the energy associated with the turbulence is continuously "injected" at low spatial frequencies and continuously cascades through the spatial frequency domain toward higher and higher spatial frequencies. Viscous dissipation, which is more severe the higher the spatial frequency, eventually "consumes" all of this turbulent flow energy, limiting the cascade to this energy to some highest possible spatial frequency. Thus the turbulence can be characterized by a lower spatial frequency limit, at which the energy is introduced, and a high spatial frequency limit, beyond which because of viscous dissipation there is no energy available to support the turbulent flow. It is customary to refer to the wavelength, L_o , associated

https://doi.org/10.1017/S0252921100118639 Published online by Cambridge University Press

with this lower spatial frequency limit, $2\pi/L_0$, as the outer scale of turbulence, and to call the wavelength, ℓ_0 , that goes with the upper spatial frequency limit, $2\pi/\ell_0$, the inner scale of turbulence.

Taking note of the fact that the rate of viscous dissipation rises rapidly with increasing spatial frequency, it was reasoned by Kolmogorov[1] that essentially all of the viscous dissipation occurred at the highest spatial frequencies. He argued that in the broad range of spatial frequencies between $2\pi/L_0$ and $2\pi/\ell_0$, which he called the inertial subrange, viscous dissipation, (and the viscosity coefficient of the fluid), played no significant part in determining the turbulent flow pattern. He was then able to show, from dimensional considerations <u>alone</u>, that the mean square difference of flow velocity at two points in space, $\vec{r}_1$ and $\vec{r}_2$, will vary as the two-thirds power of the distance between the two points. He referred to this mean square difference of velocities as the velocity structure function,

$$D_V(\vec{r}_1, \vec{r}_2) = \langle |\vec{V}(\vec{r}_1) - \vec{V}(\vec{r}_2)|^2 \rangle \quad , \tag{1}$$

were $\vec{V}(\vec{r})$ is the flow velocity vector at position $\vec{r}$, and the angle brackets denote an ensemble average. His dimensional analysis allowed him to write for the velocity structure function

$$D_V(\vec{r}_1, \vec{r}_2) = C_V^2 \, |\vec{r}_1 - \vec{r}_2|^{2/3} \quad , \tag{2}$$

where C_V^2 is introduced as a constant of proportionality and referred to as the velocity structure constant. Perhaps the most significant aspect of this result, beyond the two-thirds power dependence, <u>per se</u>, is that there apparently is no characteristic length in the inertial subrange!

https://doi.org/10.1017/S0252921100118639 Published online by Cambridge University Press

The Kolmogorov dimensional analysis provides us with virtually all of our relevant knowledge of the spatial distribution statistics of turbulence, as far as work in optical propagation is concerned. But this theory refers to the statistics of velocity fluctuations in turbulence — and velocity fluctuations, per se, do not effect optical propagation! In fact, it is possible to have strong mechanical, (i.e., velocity fluctuation), turbulence with essentially no optical effects. What couples atmospheric turbulence to optical propagation is temperature (and thus density and refractive-index) fluctuations induced by the turbulent mixing of "parcels" of warmer air from lower/higher altitudes with "parcels" of cooler air from higher/lower altitudes.

To couple the statistics of this random temperature mixing to the Kolmogorov statistics of turbulent velocity, the concept of a "conserved passive additive" was introduced by Tatarski[2] He argued that, although it was not strictly correct to consider the vertical gradient of mean atmospheric temperature as a passive additive, (since the vertical gradient can, itself, give rise to convective turbulence cells), it was a reasonable approximation to consider the variations in temperature to be a conserved passive additive. Accordingly, we would expect the difference of the local atmospheric temperature at two points to have a mean square value that was proportional to the two-thirds power of the distance between the two points. Thus Tatarski reasoned that the temperature structure functions,

$$D_T(\vec{r}_1, \vec{r}_2) = \langle [T(\vec{r}_1) - T(\vec{r}_2)]^2 \rangle \quad , \tag{3}$$

could be written as

$$D_T(\vec{r}_1, \vec{r}_2) = C_T^2 \, |\vec{r}_1 - \vec{r}_2|^{2/3} \quad , \tag{4}$$

https://doi.org/10.1017/S0252921100118639 Published online by Cambridge University Press

where C_T^2 is a constant of proportionality called the temperature structure constant. Experimental evidence[3] bears out the general validity of Tatarski's argument concerning the treatment of the atmospheric temperature gradient as a conserved passive additive. The mean square difference of atmospheric temperature measured at two points is observed to vary as the two-thirds power of the separation.

The magnitude of the temperature structure constant, C_T^2, is proportional to the local vertical temperature gradient, and thus C_T^2 can be almost zero despite the fact that the local wind velocity turbulence is quite strong — and conversely, the temperature structure constant can be relatively large under conditions where the wind velocity turbulence is weak. The magnitude of C_T^2 and of C_V^2 are not significantly coupled.

Since atmospheric density, and thus the refractive-index, are inversely proportional to atmospheric temperature, it follows from Eq. (4), together with the fact that we are dealing with small perturbations in the absolute temperature, that the mean square difference of refractive-index at two points $\vec{r}_1$ and $\vec{r}_2$, called the refractive-index structure function,

$$D_N(\vec{r}_1, \vec{r}_2) = \langle [n(\vec{r}_1) - n(\vec{r}_2)]^2 \rangle \quad , \tag{5}$$

where $n(\vec{r})$ is the refractive-index at position $\vec{r}$, can be written as

$$D_N(\vec{r}_1, \vec{r}_2) = C_N^2 \, |\vec{r}_1 - \vec{r}_2|^{2/3} \quad . \tag{6}$$

Here C_N^2 is a constant of proportionality called the refractive-index structure constant. It is our basic measure of the optical strength of atmospheric turbulence. It can, of course, vary from place to place and with time, though generally not too rapidly*. In Fig. 1 we show a sample

---

* It is of interest to note that for microwave propagation not only temperature but also water vapor play a role in determining (continued on next page)

https://doi.org/10.1017/S0252921100118639 Published online by Cambridge University Press

of the temporal variation of the path-average refractive-index structure constant as measured by Wang, et al [4] over a relatively short path near the ground.

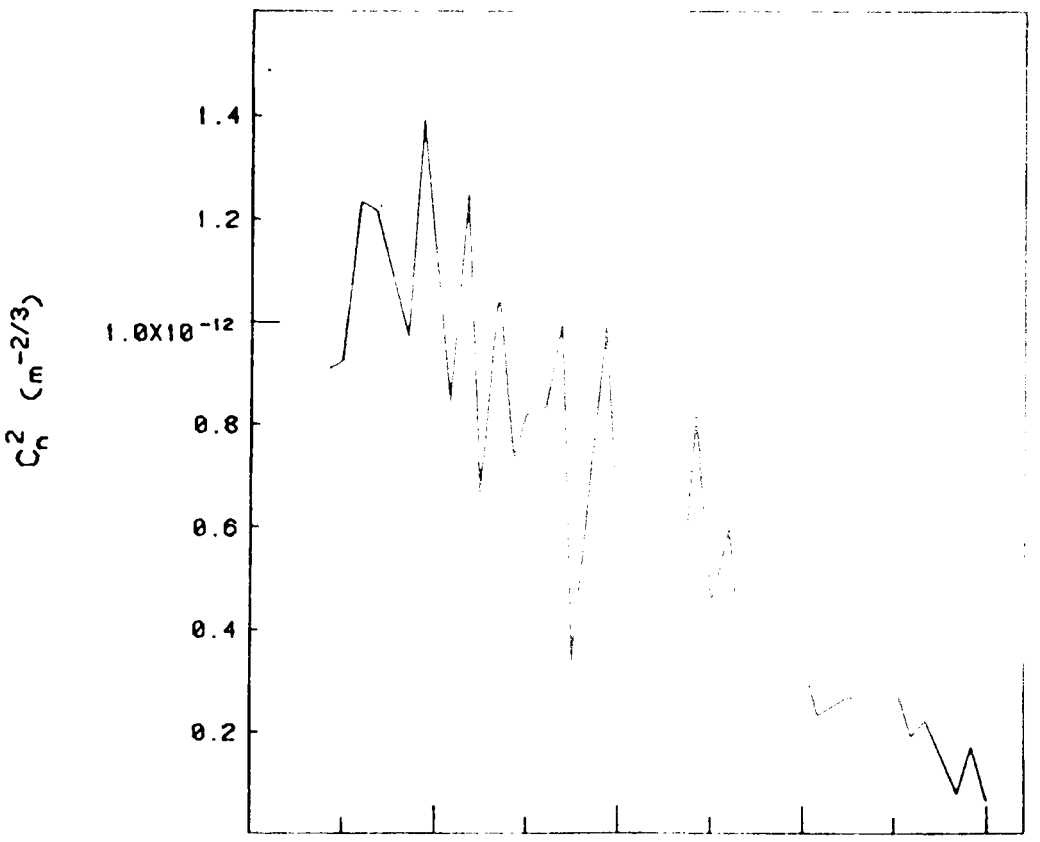

Figure 1. Time Dependence of the Refractive-Index Structure Constant Near the Ground.

Results represent the average value of C_N^2 over a 500 m path, (at a height of 1.5 m), and over a 5 minute interval. (From Ting-i Wang, G. R. Ochs, and S. F. Clifford [4].)

---

the refractive-index. However, the water vapor relative density, like the temperature varies with altitude and so is mixed as a conserved passive additive just like temperature. It follows from this this that Eq. (6) remains valid for microwave as well as optical (and infrared) propagation. The value of the refractive-index structure constant, C_N^2, will, however, vary with the wavelength of the electromagnetic radiation.

https://doi.org/10.1017/S0252921100118639 Published online by Cambridge University Press

In Fig. 2 we show what we believe is currently our best estimate of the nominal value of the refractive-index structure constant as a function of altitude. This data was assembled by Greenwood[5]. This data for the vertical distribution of C_N^2 is merely our current best estimate. We are by no means certain that these are accurate estimates of the mean value of C_N^2 at each altitude and we have no basis for estimating such things as the variability of C_N^2 with time or with geographic position either synoptically or locally. A significant amount of data gathering remains to be done in this area. Our certainty of the value of even the mean value of C_N^2 at altitudes above 10 km is particularly weak. Nonetheless, Eq. (6) and data such as that in Fig. 2 provide the basis for the existing analysis of the effects of atmospheric turbulence on optical propagation.

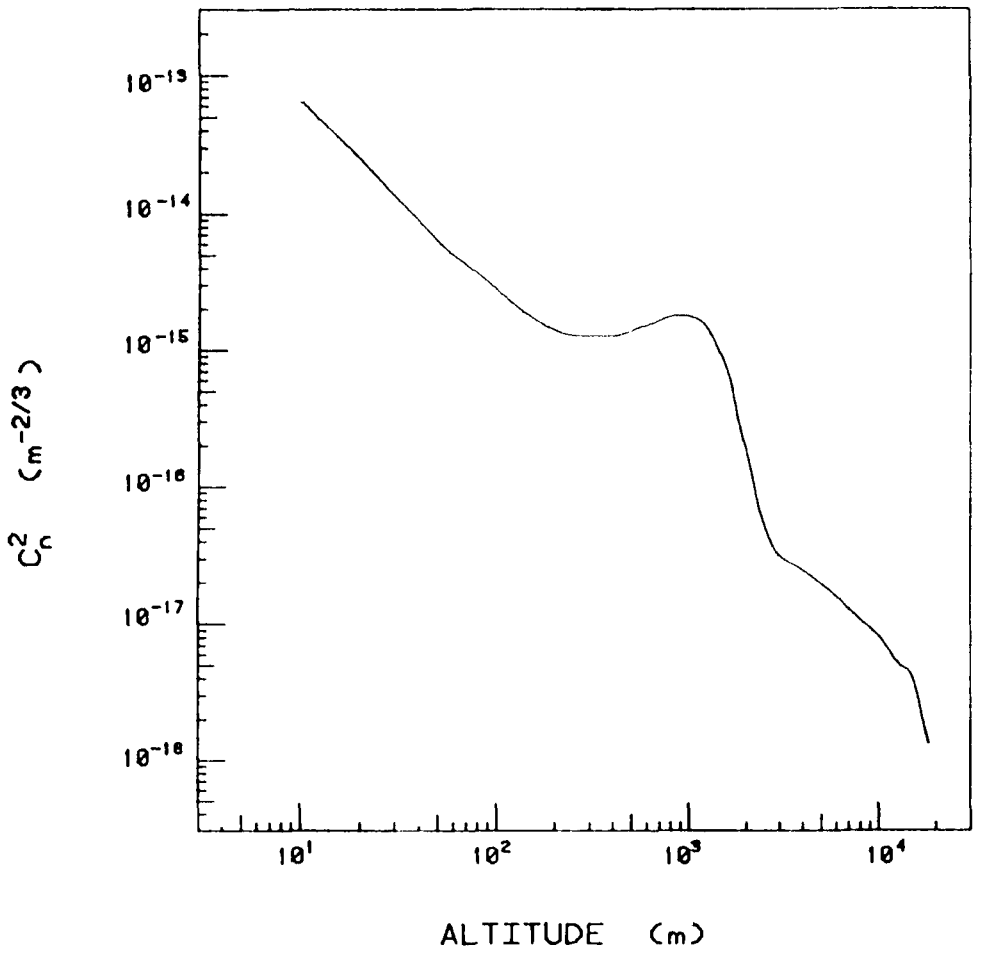

Figure 2. Vertical Distribution of the Refractive-Index Structure Constant.

(From data assembled by D. Greenwood.[5])

https://doi.org/10.1017/S0252921100118639 Published online by Cambridge University Press

Before we leave this subject of the turbulence statistics to take up the matter of propagation effects it is worth remarking on certain facts. First, we recall that Eq. (2) and thus Eq. (6) are both only valid within the inertial subrange, i.e., when

$$\ell_0 < |\vec{r}_1 - \vec{r}_2| < L_0 \tag{7}$$

For pairs of points, $\vec{r}_1$ and $\vec{r}_2$, closer together than ℓ_0 we expect very little variation in refractive-index, while for pairs of points farther apart than L_0 we have no well founded idea of what the mean square difference of refractive-index is. The size of the inner scale turbulence, ℓ_0 , depends on such things as the local kinematic viscosity and the rate at which energy is delivered to the turbulent process. Though it varies with locality and with altitude, it is generally estimated that ℓ_0 is of the order of one or two centimeters or less. Near the ground the outer scale of turbulence, L_0 , may be only a few meters in size but at higher altitudes there is evidence that it can be hundreds of meters in size, or even larger.

Second, it is worth recalling that within the inertial subrange there is no natural scale size characterizing the turbulence! This, in effect, prevents us from developing any analytically more tractable expression for the refractive-index structure function, $D_N(\vec{r}_1 - \vec{r}_2)$, than Eq. (6). While characteristic scale sizes for such things as wavefront distortion can be developed these depend on such other things as the wavelength and the propagation path length and so, although they are length scales, they are not characteristic of the turbulence, per se .

Third, it is worth remarking on the two-thirds power law. This power law arises as a direct consequence of Kolmogorov's dimensional analysis. Though this particular power law seems a bit unusual it should be noted that a three-thirds power law would represent nothing more than

https://doi.org/10.1017/S0252921100118639 Published online by Cambridge University Press

a random walk. Apparently the turbulent mixing process results in a bit more correlation than a random walk. The presence of the two-thirds power law governing the refractive-index variations will make itself felt in the propagation results where we shall see other fractional powers such as five-thirds, seven-sixths, eleven-sixths, etc. All of these would have much more ordinary values if the two-thirds power in Eq. (6) were a unity power.

Fourth and finally, it is worth remarking on the use of the structure function rather than a correlation function to define the turbulence statistics and the refractive-index statistics. This is directly related to the fact that we know nothing about the very low spatial frequencies in the turbulence. With our inability to place a bound on the contribution of these low spatial frequencies to the random velocity or refractive-index variations we have, in effect, allowed the variance to have an infinite value. Fortunately, this infinite standard deviation has no physically observable implications in our propagation calculations and in that sense, the infinite variances can be ignored. From a mathematical point of view the use of the structure function, (rather than the use of a correlation function), has the explicit effect of allowing us to ignore this infinite standard deviation. The value of the structure function does not go to infinity except for infinitely large separations between $\vec{r}_1$ and $\vec{r}_2$, a case of no concern to us here.

3. WAVEFRONT DISTORTION STATISTICS

Wavefront distortion statistics are generally measured in terms of the mutual coherence function, a quantity calculated directly from the electromagnetic field function, per se, or else in terms of the log-amplitude, phase, and wave structure functions — quantities calculated from the complex phase shift denoting the wavefront's intensity and phase variations induced by turbulence. We shall restrict our attention to these latter quantities, and work with the statistics of the complex phase. We may

https://doi.org/10.1017/S0252921100118639 Published online by Cambridge University Press

define the complex phase shift, $\psi(\vec{r})$, at position $\vec{r}$ on a plane nominally parallel to the wavefront, by the equation

$$u(\vec{r}) = u_0(\vec{r}) \exp [i \psi(\vec{r})] \quad , \tag{8}$$

where $u_0(\vec{r})$ is the wavefront that would exist at $\vec{r}$ if there were no turbulence in the propagation path, and $u(\vec{r})$ is the randomly distorted wavefront that actually exists because of the random turbulence pattern in the propagation path.

The complex phase, $\psi(\vec{r})$, can be separated into real and imaginary parts corresponding to the ordinary phase shift, $\phi(\vec{r})$, and the log-amplitude, $\ell(\vec{r})$. We can write,

$$\psi(\vec{r}) = \phi(\vec{r}) + i \ell(\vec{r}) \quad . \tag{9}$$

Theoretical arguments[2] confirmed by experimental evidence[6,7] indicates that both the ordinary phase shift and the log-amplitude are Gaussian random variables. The statistical quantities of interest to us are the second moments as measured by the structure function, namely the log-amplitude structure function,

$$D_\ell(\vec{r}_1 - \vec{r}_2) = \langle [\ell(\vec{r}_1) - \ell(\vec{r}_2)]^2 \rangle \quad , \tag{10}$$

the ordinary phase structure function,

$$D_\phi(\vec{r}_1 - \vec{r}_2) = \langle [\phi(\vec{r}_1) - \phi(\vec{r}_2)]^2 \rangle \quad , \tag{11}$$

and the wave structure function

$$D_\psi(\vec{r}_1 - \vec{r}_2) = \langle |\psi(\vec{r}_1) - \psi(\vec{r}_2)|^2 \rangle \quad . \tag{12}$$

https://doi.org/10.1017/S0252921100118639 Published online by Cambridge University Press

It can be shown that the wave structure function is just the sum of the log-amplitude and the ordinary phase structure functions, i.e.,

$$D_\psi(\vec{r}_1 - \vec{r}_2) = D_\ell(\vec{r}_1 - \vec{r}_2) + D_\phi(\vec{r}_1 - \vec{r}_2) \quad . \tag{13}$$

In analysis of the performance of various imaging and pseudo imaging concepts it is found that so long as the process does not involve fourth moments of the wavefunction, then the wave structure function provides a complete definition of the relevant statistics of turbulence effects. This is the quantity of basic interest to us. We find that in most all propagation scenarios of interest the log-amplitude structure function is small compared to the phase structure function. Moreover, we find that if we calculate the phase structure function, D_ϕ, ignoring those diffraction/interferences effects which give rise to intensity variations the result is identical to the wave structure function, D_ψ. Accordingly, it is generally quite accurate to ignore intensity variations in analysis of wavefront distortion sensitive systems, and use the ordinary phase structure function calculated in accordance with this suppression of intensity effects, as though it completely defined the wavefront distortion statistics. This not only greatly simplifies the system analysis, but also insures the easy interpretability of the results. Accordingly, we shall proceed in this way in all of the following.

For propagation from a point source at range, R, to an aperture plane on which we define a two-dimensional position vector, $\vec{r}$, it can be shown[8] that the phase structure function is

$$D_\phi(\vec{r}) = \{2.91\, k^2 \int_0^R ds\, C_N^2\, (s/R)^{5/3}\}\, r^{5/3} \quad . \tag{14}$$

Here the variable of integration, s, runs along the propagation path taking the value 0 at the point source and the value R at the aperture plane. The refractive-index structure constant, C_N^2, can vary along the propagation

https://doi.org/10.1017/S0252921100118639 Published online by Cambridge University Press

path. The quantity k denotes the optical wave-number, $2\pi/\lambda$ In the case of an infinite plane wave source Eq. (14) is replaced[2] by the expression,

$$D_\phi(\vec{r}) = \{2.91\, k^2 \int_0^R ds\, C_N^2\}\, r^{5/3} \quad , \tag{15}$$

which is the expression of basic interest to us in considering propagation of star light down through the atmosphere. [It is perhaps worth noting that Eq. (15) can be easily obtained from Eq. (14) by considering, instead of an infinite plane wave source at the origin, a point source at minus infinity and a turbulence free propagation environment, (i.e., $C_N^2 = 0$), from minus infinity to the origin.] The significant thing about these expressions for the phase structure function is the $r^{5/3}$ dependence, the five-thirds power deriving its form directly from the two-thirds power dependence of the refractive-index structure function of Eq. (6)

It is convenient[9] to define a length ρ_o in accordance with the equation

$$\rho_o = \{2.91\, k^2 \int_0^R ds\, C_N^2\, (s/R)^{5/3}\}^{-3/5} \quad , \tag{16}$$

for a point source, or as

$$\rho_o = \{2.91\, k^2 \int_0^R ds\, C_N^2\}^{-3/5} \quad , \tag{17}$$

for an infinite plane wave source. With the length ρ_o so defined we can write the phase structure function for both cases as

$$D_\phi(\vec{r}) = (r/\rho_o)^{5/3} \quad . \tag{18}$$

It should be noted that while the turbulence in the inertial subrange lacked a length scale, the introduction of a propagation path length, R , and of an optical wavelength, λ , makes it possible to define a length scale characteristic of turbulence induced wavefront distortion.

https://doi.org/10.1017/S0252921100118639 Published online by Cambridge University Press

For our purposes the length scale, ρ_0 , is not the most convenient that could be defined. It can be shown[10] that if we are interested in the effect of wavefront distortion on circular aperture optical systems then the quantity, r_0 , defined by the equation

$$r_0 = [2^{6/5} \sqrt{\Gamma (11/5)}\,]\, \rho_0$$

$$\approx (6.88)^{3/5}\, \rho_0 \quad , \tag{19}$$

is a basically more convenient property. Using r_0 in place of ρ_0 we rewrite the phase structure function of Eq. (18), as

$$D_\phi (\vec{r}) = 6.88\, (r/r_0)^{5/3} \quad . \tag{20}$$

The convenience of the use of r_0 derives from the fact that it "represents" an aperture diameter for which the conventional optical system diffraction limits on an infinite diameter optical system. Anticipating results which will be discussed in more detail later, in Fig. 3 we show the turbulence limited resolution of a conventional imaging system. As can be seen, the resolution achieved by a very large aperture system in the presence of turbulence is just equal to the resolution that would be achieved if the aperture diameter were r_0 , but there were no turbulence induced wavefront distortion.

Another way to infer the practical physical significance of the coherence diameter, r_0 , is to note, as will be discussed later, that over a circular aperture of diameter r_0 the rms wavefront distortion is almost exactly one radian. Because of its obvious direct physical significance in optical system performance, we shall generally use r_0 as our measure of wavefront distortion.

https://doi.org/10.1017/S0252921100118639 Published online by Cambridge University Press

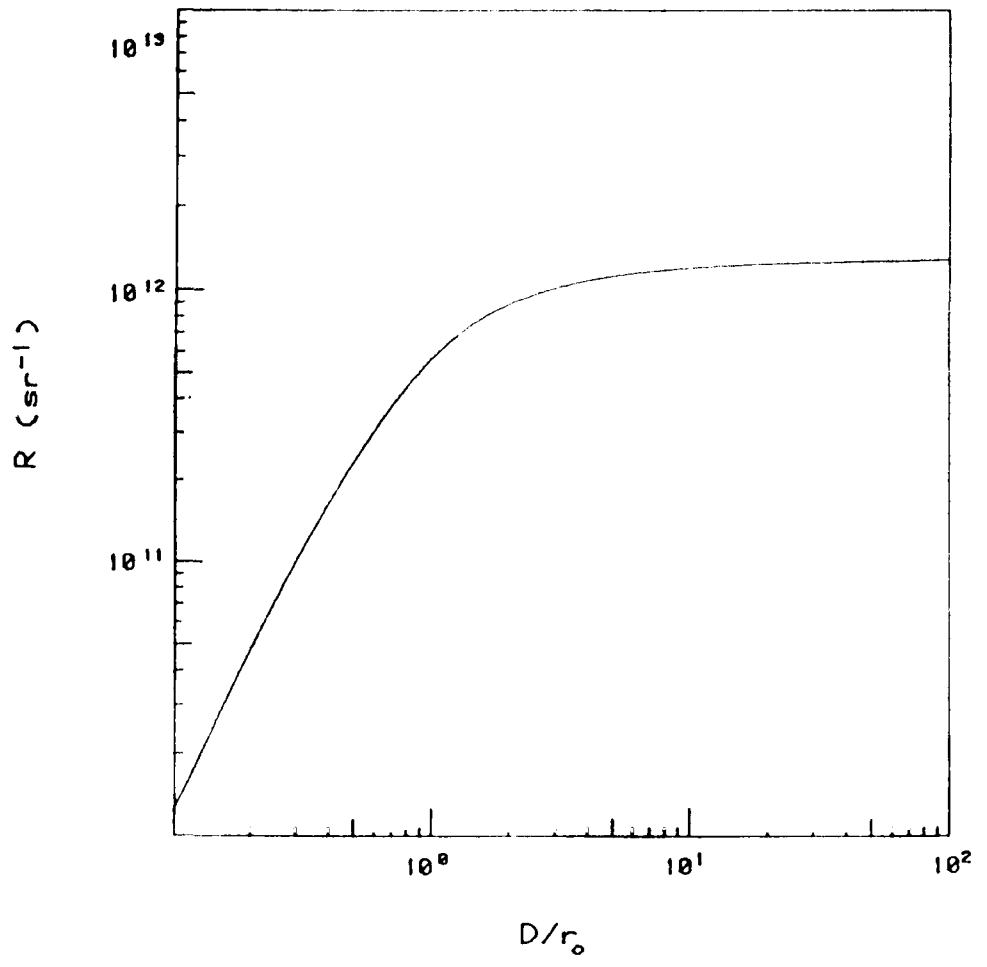

Figure 3. Resolution of a Turbulence Limited Optical System as a Function of Aperture Diameter.

The aperture diameter, D, is normalized by dividing by r_o. Resolution, R, (measured in inverse steradians), can be thought of as antenna gain or the inverse of transmitter or receiver beam width. For values of aperture diameter smaller than r_o the resolution to the square of asymptotically approaches proportionality the diameter, which corresponds to diffraction limited performance. For diameters much larger than r_o the resolution is virtually independent of the diameter and asymptotically approaches a value of 1.27×10^{12} sr^{-1}, corresponding to $\lambda = 0.55 \times 10^{-6}$ m and $r_o = 0.07$ m. The knee of the curve, i.e., the point of intersection of the two asymptotic curves, (i.e., straight lines) occurs at $D = r_o$.

The turbulence limited optical resolution is clearly of the order of λ/r_o. Making use of Eq.'s (16) or (17) and Eq. (19), we can see that the coherence diameter, r_o, is proportional to, $\lambda^{6/5}$, the wavelength to the six-fifths power. From this, it follows that the turbulence limited angular resolution, λ/r_o, is proportional to $\lambda^{-1/5}$. The turbulence limited resolution of conventional imaging is almost, but not quite, independent of wavelength. Between the visible and ten micron region there is a factor of $(0.55 \times 10^{-6}/10.0 \times 10^{-6})^{-1/5} = 1.79$ difference in the turbulence limited angular resolution. With a large enough aperture we obtain almost twice

https://doi.org/10.1017/S0252921100118639 Published online by Cambridge University Press

as good resolution at the longer wavelength — though what constitutes large enough apertures differ by a factor of $(10.0 \times 10^{-6} / 0.55 \times 10^{-6})^{6/5} = 32.5$ in diameter between the two wavelengths.

Before leaving this section it is useful to apply the data of Fig. 2 to a calculation of a nominal value of r_0 . Simple numerical quadrature indicated that for the data of Fig. 2,

$$\int_0^\infty ds\, C_N^2 = 3.57 \times 10^{-12} \text{ , } m^{1/3} \text{ ,} \tag{21}$$

so that

$$r_0 = 0.0420\, (\lambda / 0.55 \times 10^{-6})^{6/5} \text{ , m .} \tag{22}$$

This value is only in fair to poor agreement with our general observation, corresponding as it does to $\lambda / r_0 = 13.1$ μrad in the visible.

The coherence diameter, r_0 , is not a constant but rather a slowly changing random variable. Experimental evidence[11] based on measurements of the width of the image of a star, shows that from night to night the value of the coherence diameter fluctuates as a log-normal random variable with a medium value of $r_0 = 0.0752$ m for zenith viewing at a wavelength of $\lambda = 0.55 \times 10^{-6}$ m*. The log-normal distribution for r_0 is such that a one-sigma deviation corresponds to a change in the value of r_0 by a factor of 1.36 , i.e., about 16% of the time we expect r_0 to be larger than $1.36 \times 0.0752 = 0.102$ m, and 16% of the time we expect it to be smaller than $0.0752/1.36 = 0.0553$ m. These values apply about equally well to the two observatory sites at which the measurements were made.

---

* The difference between this value of r_0 (i.e., 0.0752 m) and the value (0.0420 m) calculated from the data in Fig. 2 may simply reflect the difference between sites.

https://doi.org/10.1017/S0252921100118639 Published online by Cambridge University Press

If the strength of turbulence varies significantly with the site, then different values may apply elsewhere.

With these results defining wavefront distortion statistics thus in hand we are now ready to take up the questions of providing a geometric interpretation of the wavefront distortion. This is presented in the rather brief next section.

4. WAVEFRONT DISTORTION GEOMETRY

At first it would seem impossible to discuss in a quantitative manner the "shape" of the randomly distorted wavefront. All that we would seem to be able to say is that the wavefront is distorted with some mean square deviation between pairs of points of various separations. In fact, however, we can apply quantitative techniques to the assessment of the shape. This is done by considering a circular region of diameter D, within which we wish to analyze the statistics of wavefront shape. At any instant we have a circular sample of the randomly distorted wavefront. Using a set of functions defined so as to be orthonormal over the circle we can decompose the random wavefront sample. We obtain a set of coefficients, one for each of the orthonormal functions, which taken together define the wavefront shape. Just as the distorted wavefront is a random function, these coefficients are random variables. We can calculate the mean square value of these coefficients from our knowledge of the phase structure function.[12]

In order to be able to associate shapes with these random coefficients and their mean square values, it is convenient to choose the series of orthonormal functions to correspond to polynomials of increasing order. The preferred choice is the Zernike polynomials, for which the first term in the series is constant over the circular aperture, the next two correspond to the two degrees-of-freedom to be associated with the concept of tilt, and the next three to spherical (i.e., focus) and the two degrees-of-freedom of

https://doi.org/10.1017/S0252921100118639 Published online by Cambridge University Press

cylindrical shaped wavefront distortion (i.e.,"astigmatism"). The mean square values of the random coefficients associated with these functions define the amount of tilt, of focus error, and of cylindrical wavefront distortion in the wavefront's shape. It can be shown that the ratio mean square strength of tilt-to-focus-to-cylindrical shaped wavefront error is as 1/0.0239/0.0521, or measured per degree of freedom, as 1/0.0478/0.0521. Clearly the tilt aspect of the wavefront distortion shape is the dominant aspect of the shape. Detailed analysis[13] extending to very high order Zernike polynomials has shown that none of the higher order wavefront distortion shapes is any more significant than the spherical (focus) or cylindrical shapes.

A somewhat different view of the problem, but leading to the same conclusion, i.e., the dominance of the tilt aspect of the wavefront distortion , is obtained if we consider the residual wavefront error, if we had adaptive optics capable of perfectly compensating for various of the lower order wavefront distortion shapes. With no adaptive optics type correction, (except to ignore the fluctuation in time of the average phase across the circular aperture), the mean square (residual) wavefront distortion will be

$$\Delta_1 = 1.030\,(D/r_0)^{5/3} \quad . \tag{23}$$

If the adaptive optics can compensate for the random wavefront tilt, then the residual error will be

$$\Delta_3 = 0.134\,(D/r_0)^{5/3} \quad . \tag{24}$$

If tilt and focus errors are corrected , the residual wavefront error will be

$$\Delta_4 = 0.111\,(D/r_0)^{5/3} \quad . \tag{25}$$

https://doi.org/10.1017/S0252921100118639 Published online by Cambridge University Press

If the correction compensates all wavefront distortion shapes that are linear or quadratic in nature, the residual wavefront distortion error will be

$$\Delta_8 = 0.0648\,(D/r_0)^{5/3} \quad . \tag{26}$$

With all cubic shapes also included in the correction, the residual error will be

$$\Delta_9 = 0.0463\,(D/r_0)^{5/3} \quad , \tag{27}$$

while if the correction can also accomodate quartic shapes, the residual wavefront distortion error will be

$$\Delta_{13} = 0.0328\,(D/r_0)^{5/3} \tag{28}$$

Clearly, the major reduction in the residual wavefront error is that produced when we correct for the random tilt. Correcting with the two degrees-of-freedom associated with tilt gives a reduction in the residual wavefront error of $\Delta_1/\Delta_3 = 7\ 69$, while the next ten degrees-of-freedom only provide a further reduction of the residual wavefront error of $\Delta_3/\Delta_{13} = 4.09$.

It is significant to note that in many cases random tilt is not observable during a period shorter than that in which the wavefront distortion changes. For such cases the correction for tilt is in a sense automatic. It is useful to note that while the mean square wavefront error with no tilt correction is $\Delta_1 = 1.030\,(D/r_0)^{5/3}$, if tilt is corrected, the residual error is

$$\Delta_3 = 1.030\left(\frac{D}{3.40\ r_0}\right)^{5/3} \quad . \tag{29}$$

When the tilt shaped portion of the wavefront distortion can be ignored, (as for example, in short exposure imagery), a substantial increase in the allowable aperture diameter is possible for the same mean square residual wavefront error.

https://doi.org/10.1017/S0252921100118639 Published online by Cambridge University Press

With this presentation of the shape analysis of wavefront distortion in hand, and with the major role of random wavefront tilt thus clearly indicated, we are now ready to turn to an examination of conventional imaging systems. We take this up in the next section.

5. CONVENTIONAL IMAGERY

In the analysis of the quality and resolution of conventional imagery, it is customary to approach the problem from the point of view of the optical transfer function. For our purposes, the simplest definition of the optical transfer function is that it is the Fourier transform of the image of a unit strength point source. Inasmuch as the image is defined on a two-dimensional (focal plane) space, $\vec{\theta}$, the Fourier transform and the spatial frequency, $\vec{f}$, must also be two-dimensional. As a matter of convenience, we shall consider the focal plane space to be measured in an angular coordinate system corresponding to the optical system's field-of-view space. Accordingly, the spatial frequency space is measured in units of cycles per radian field-of-view.

It is well established[14,15] that for conventional long-exposure imagery with a circular aperture of diameter D operating at a wavelength λ , the optical transfer function at spatial frequency $\vec{f}$ is

$$\tau_{LE}(\vec{f}) = \tau_{DL}(\vec{f}) \exp\left[-\tfrac{1}{2} D_{\phi}(\lambda\vec{f})\right]$$

$$= \tau_{DL}(\vec{f}) \exp\left[-3.44\,(\lambda f/r_o)^{5/3}\right] \quad , \tag{30}$$

where $\tau_{DL}(\vec{f})$ is the diffraction-limited transfer function of the imaging system, with value given by the expression

$$\tau_{DL}(\vec{f}) = \frac{2}{\pi}\left\{\cos^{-1}\left(\frac{\lambda f}{D}\right) - \left(\frac{\lambda f}{D}\right)\left[1 - \left(\frac{\lambda f}{D}\right)^2\right]^{1/2}\right\} . \tag{31}$$

https://doi.org/10.1017/S0252921100118639 Published online by Cambridge University Press

We can see from a consideration of Eq (30) that the spatial frequency $\vec{f}$ can be associated with a distance, $\vec{r}_1 - \vec{r}_2 = \lambda\vec{f}$, on the aperture. The degradation of the optical transfer function from its diffraction-limited value is a function of the mean square phase difference for that separation distance.

For a short exposure image, the random wavefront tilt will displace the image of a point source, but it will not blur it. There will, of course, be some amount of blurring of the image, but this will be due to the higher order shapes in the wavefront distortion. If we ignore/suppress the random displacement of the image and take the average of a series of short exposures, it can be shown[15] that the resultant point source image gives rise to a short exposure optical transfer function which can be written as

$$\tau_{SE}(\vec{f}) = \tau_{DL}(\vec{f}) \exp\{-3.44\,(\lambda f/r_o)^{5/3}\,[1 - (\lambda f/D)^{1/3}]\} \quad . \qquad (32)$$

The term in the square brackets represents the tilt suppression effect.

A particularly interesting way to consider the overall imaging performance of a conventional imaging system is to define the resolution of the system as the integral of the optical transfer function over the spatial frequency domain. Since the optical transfer function is normalized to unity at $\vec{f} = 0$ (i.e., at d.c.), the resolution so defined is a measure of the "bandwidth" of the imaging system. Because the spatial frequency is a two-dimensional vector, the integration should also be two-dimensional. Thus the resolution has the dimensions of inverse steradians, corresponding to one over the "resolution beam width".

We define the resolution by the equation

$$\mathcal{R} = \int d\vec{f}\ \tau(f) \quad . \qquad (33)$$

https://doi.org/10.1017/S0252921100118639 Published online by Cambridge University Press

It can be shown that for a very large diameter circular aperture long exposure imaging system, the resolution is

$$\mathcal{R}_\infty = \tfrac{1}{4}\pi\,(r_0/\lambda)^2 \quad . \tag{34}$$

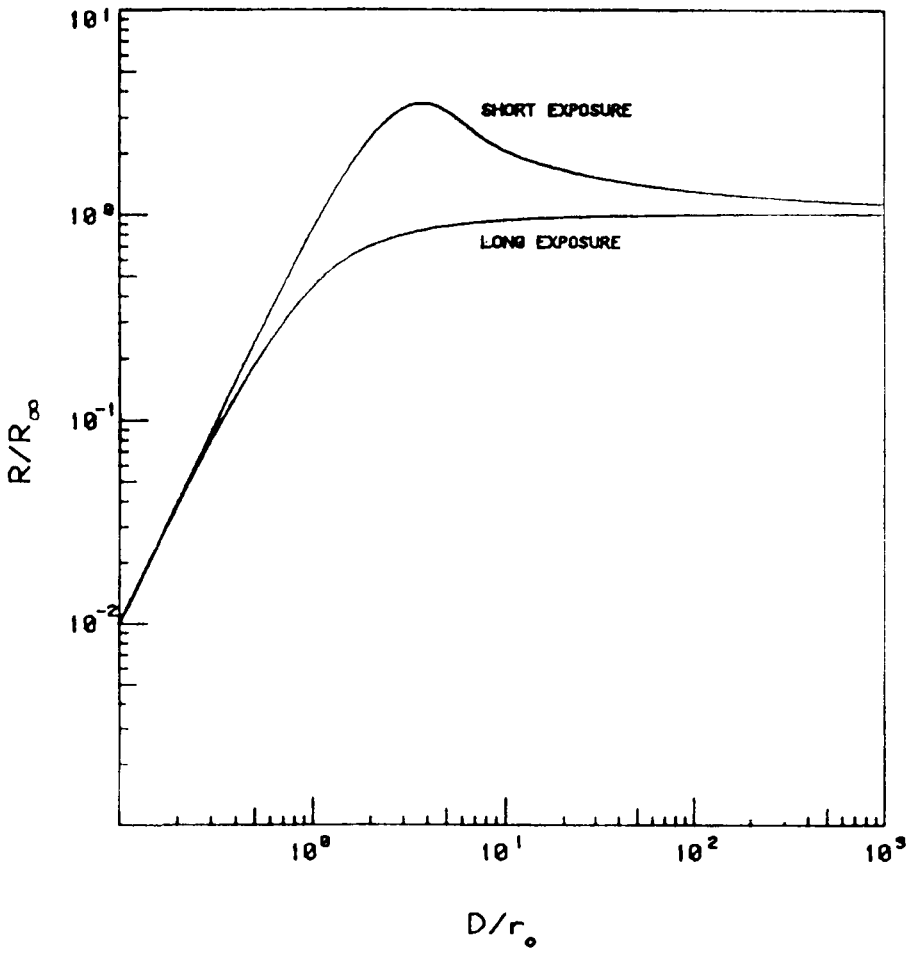

Figure 4. Normalized Resolution as a Function of Normalized Aperture Diameter for Very Long and Very Short Exposures.

The resolution normalization factor is $\mathcal{R}_\infty = \frac{1}{4}\pi\,(r_0/\lambda)^2$

In Fig. 4, we show normalized resolution, $\mathcal{R}/\mathcal{R}_\infty$, as a function of normalized aperture diameter, D/r_0, for both long and short exposure imagery. In general, the results speak for themselves. However, it is perhaps worth noting that the peak of the short exposure curve occurs rather near $D \approx 3.4\ r_0$ — a fact interesting in its relationship to Eq. (29). The decrease in the short exposure resolution as larger aperture diameters are considered may be attributed to the fact that for these very large diameters, the wavefront distortion components of higher order than tilt are large enough that they, themselves, can limit the resolution.

https://doi.org/10.1017/S0252921100118639 Published online by Cambridge University Press

Before leaving the subject of resolution for a conventional imaging system, it is worthwhile to consider the optical transfer function that is to be associated with a Michelson stellar interferometer system. Such a system can be considered to be an imaging system, except that the spatial frequencies associated with the separation of the two apertures may be "translated" to an apparently different spatial frequency on the image plane. If the separation of the two apertures is L and the diameter of each aperture is D, then the system will have a non-zero optical transfer function for spatial frequencies with magnitude less than D/λ, and those spatial frequencies around (i.e., with a distance D/λ of) $\pm \vec{L}/\lambda$. It is only these spatial frequencies around $\pm \vec{L}/\lambda$ that are of any real interest.

For short exposure operation of the interferometer, the optical transfer function at frequency $\pm \vec{L}/\lambda$ will be of the order of

$$\tau(\pm \vec{L}/\lambda) \approx \tfrac{1}{2} \exp(-2\Delta_1)$$

$$\approx \tfrac{1}{2} \exp\left[-2.06\,(D/r_0)^{5/3}\right] \quad . \qquad (35)$$

It should be noted that $2\Delta_1$ is the mean square random phase difference between pairs of points, one in each of the two apertures of the interferometer. This fact is the basis for writing Eq. (35). [The reason Δ_1 rather than Δ_3 appears in Eq. (35), even though this is a short exposure problem, is that the system is sensitive to wavefront tilt within each of the two apertures. If the two tilts are not equal, fringe contrast is lost.] The factor of one-half in Eq. (35) simply has to do with the d.c. normalization. For high contrast fringes, it is obvious that the diameter of the individual apertures, D, must be less than the coherence diameter, r_0.

For long exposure operation, the transfer function will be of the order of $\tfrac{1}{2} \exp\left[-3.44\,(L/r_0)^{5/3}\right]$. Clearly, for any interesting aperture separation distance, L, the transfer function will be very small and there will

https://doi.org/10.1017/S0252921100118639 Published online by Cambridge University Press

be essentially no fringe contrast. It will provide useful insight into speckle techniques for us to consider here why the optical transfer function for long exposure is so much poorer than for short exposure operation of a Michelson stellar interferometer, and to consider why the short exposure operation of the interferometer gives so much better an optical transfer function than we would obtain at the same spatial frequency with a lens whose diameter was large enough to accommodate that same spatial frequency.

For long exposure operation of the interferometer, at each instant, assuming that the individual apertures are relatively small, i.e., that $D \ll r_0$, there is a sharp sinusoidal intensity pattern on the focal plane corresponding to the spatial frequencies $\pm \vec{L}/\lambda$. The phase of this sinusoidal intensity pattern is equal to some constant plus the phase difference associated with the wavefront at the two apertures. As the randomly changing wavefront distortion changes this phase difference, the phase of the sinusoidal intensity pattern will vary and the pattern will appear to shift back and forth. For a change in the phase difference of π radians, the sinusoidal intensity pattern will shift by half of a cycle, replacing bright by dark and dark by bright. This continuous random shifting of the pattern during a long exposure period will tend to wash out the inherent contrast in the fringes. It can be shown that if the rms shift of the fringes is S (measured in fringe wavelengths), then the long exposure fringe contrast will be reduced by $\exp\left[-\frac{1}{2}(2\pi S)^2\right]$. It is this that gives rise to the factor of $\exp\left[-3.44\,(L/r_0)^{5/3}\right]$ quoted previously. The long exposure fringe loses contrast because averaging of the intensity pattern over random phase shifts drives the long exposure image to a uniform, nearly zero contrast pattern. The average is of intensity, and so the contrast is driven to zero.

In comparing short exposure imagery using a large circular aperture, with short exposure imagery using a Michelson stellar interferometer, we run into a different kind of averaging. In this case, the key matter is the

https://doi.org/10.1017/S0252921100118639 Published online by Cambridge University Press

recognition that every pair of points in the total aperture with a separation of $\lambda\vec{f}$ gives rise to a sinusoidal signal in the focal plane corresponding to the spatial frequency $\vec{f}$. Because all pairs of aperture points contribute at the same time, and because there is temporal coherence across the aperture, i.e., the electromagnetic field from different pairs of points can interfere with the field from other pairs of aperture points, we get a different kind of averaging than we did in averaging over time for a long exposure. Pairs of points that are sufficiently proximate on the aperture will produce spatially sinusoidally varying electromagnetic fields that are spatially coherent with respect to each other, providing proximity is taken to mean a separation on the aperture plane of much less than r_0 .

For a single large aperture imaging system, there are many pairs of aperture positions with separation $\lambda\vec{f}$ which pairs are not proximate to each other. If we group pairs into proximate pair groupings, we can argue that there are of the order of $(D/r_0)^2\ \tau_{DL}\ (\vec{f})$ such pairs. Within each grouping, the sinusoidal pattern generated by each pair will interfere more or less constructively with that generated by all the other pairs. However, between groupings the interferences will have a random phase shift and the resultant spatially varying sinusoidal pattern, while it will not average to zero, will only grow in intensity as the square root of the number of groupings combined. The random sum of the sinusoidal patterns gives rise to a sinusoidally varying intensity pattern which has an rms amplitude down by about a factor of $[(D/r_0)^2\ \tau_{DL}\ (\vec{f})]^{1/2}$ from the value of $\tau_{DL}(\vec{f})$ which it would have if there were no wavefront distortion and everything combined coherently. Thus, while the optical transfer function for short exposure operation of the Michelson stellar interferometer (with small individual apertures) is near unity, the short exposure optical transfer function of comparably large spatial frequencies for a very large aperture will be a random sum with an

https://doi.org/10.1017/S0252921100118639 Published online by Cambridge University Press

rms amplitude of the order of $[(r_o/D)^2\ \tau_{DL}(\vec{f})]^{1/2}$ It is to be noted that this is not the amplitude of the intensity sine wave in a sum of short exposure images, but rather is the "quadrature sum" of the amplitude of the intensity sine wave in each short exposure image. As such, it is larger than the conventional short exposure optical transfer function given by Eq. (32), and will be seen to be more directly related to a speckle system optical transfer function.

6. SPECKLE SYSTEM

The basis for understanding of speckle system performance, such as defined by Labeyrie[16] and by Knox and Thompson[17], is contained in the preceding discussion. For a large circular aperture, there are many [of the order of $(D/r_o)^2\ \tau_{DL}(\vec{f})$] groupings of pairs of aperture points contributing to the spatial frequency $\vec{f}$ in the focal plane pattern. These groupings interfere randomly with each other, producing a sinusoidal intensity pattern which is not only reduced in amplitude compared to the possible sum, but also randomly phase shifted. In the ordinary short exposure imagery concept, where we add up the several short exposure images, the random phases of the sum cause the sinusoidal intensity patterns to average to zero. In a speckle system, it is the square of the amplitudes of the sinusoidal component in each short exposure that is summed. There is no phase shift problem, and the sums accumulate constructively. As indicated previously, and as demonstrated by Korff[18], if we consider the rms amplitude of the spatial frequency as defining the optical transfer function, then we get for the (Labeyrie) speckle (interferometry) system optical transfer function

$$\tau_{SI}(\vec{f}) = \langle |\tau(\vec{f})|^2 \rangle^{1/2}$$

$$\approx 0.66\ (r_o/D)\ [\tau_{DL}(\vec{f})]^{1/2} \quad . \qquad (36)$$

https://doi.org/10.1017/S0252921100118639 Published online by Cambridge University Press

This indicates the expected amplitude of the basic signal developed by the Labeyrie speckle interferometry technique for a single large aperture.

Knowledge of these amplitudes, generated by the Labeyrie technique, allow the power spectrum and correlation function to be determined for the object being viewed. For a pair of somewhat smaller apertures, but each with diameter D significantly greater than the coherence diameter, r_o , and with a center-to-center spacing of $\vec{L}$ between the apertures, we can infer the optical transfer function for spatial frequencies of the order of $\vec{f} = \pm \vec{L}/\lambda$. We estimate the optical transfer function in this case as being

$$\tau_{s_1}(\vec{f}) = \langle |\tau(\vec{f})|^2 \rangle^{1/2}$$

$$\approx \tfrac{1}{2}(r_o/D) \quad . \tag{37}$$

This corresponds to the square-root of the number of groupings of pairs of aperture points matching the spatial frequency. The factor of one-half arises from the fact that at d.c. (very low) spatial frequencies, there are twice as many groupings of "pairs" of points, since each of the apertures contributes separately — and this defines the normalization.

For the Knox-Thompson speckle imaging technique, the amplitude of each spatial frequency is essentially the same as given by Eq. (36) for speckle interferometry. The key to the Knox-Thompson technique, that provides its ability to recover a true image rather than merely a correlation function, is the recovery of the target-object induced phase shift of each spatial frequency component. Because of the very large (i.e., several times 2π) random phase shift introduced by turbulence into each spatial frequency component in the individual image recordings, it is not possible (practical?) to try to extract the component of phase shift introduced by the object pattern from a study of the spatial frequency component as they appear in the focal plane image — at least not directly. However, it was

https://doi.org/10.1017/S0252921100118639 Published online by Cambridge University Press

noted by Knox and Thompson that for nearly equal spatial frequencies, $\vec{f}_1$ and $\vec{f}_2$, the groupings of pairs of aperture points that contribute to the one frequency are almost the same as the groupings that contribute to the other frequency, providing

$$|\vec{f}_1 - \vec{f}_2| \ll r_0/\lambda \quad . \tag{38}$$

If this condition is satisifed, then in any short exposure the turbulence-induced phase shift on the $\vec{f}_1$ component will be almost identical to that induced on the $\vec{f}_2$ component. The difference in the apparent phase of the two components for that short exposure will contain only a small contribution (i.e., much less than $\frac{1}{2}\pi$) due to turbulence. The difference in the apparent phase of the two components will be almost entirely due to the difference in the object pattern induced phase shift for these two spatial frequencies.

The Knox-Thompson algorithm involves the calculation of these phase shift differences and the averaging of the difference over many short exposures. In this average, the turbulence contributions, which varies from frame to frame but are generally less than $\frac{1}{2}\pi$, averages to zero so that the result represents only the phase difference between spatial frequency components of the object pattern. With an array (two-dimensional) of these phase difference measurements covering the entire spatial frequency domain of interest, it is then possible to "integrate" the differences to obtain an absolute phase shift to be associated with each spatial frequency.

The underlying concept behind the Knox-Thompson algorithm is basically straightforward. Our quantitative understanding of it, however, is restricted to Eq. (38) . No theory has been developed to indicate the extent to which turbulence effects are not completely compensatable in the recovered image, and for the present, we can only assume that these effects are not significant.

https://doi.org/10.1017/S0252921100118639 Published online by Cambridge University Press

With this understanding of the Labeyrie and Knox-Thompson speckle technique in hand, we are now ready to take up consideration of spectral bandwidth constraints. This is treated in the next section.

7. SPECTRAL BANDWIDTH CONSTRAINTS FOR SPECKLE SYSTEMS

No carefully developed theory for the allowable spectral bandwidth in the formation of a speckle photograph has yet been published. However, it is possible to form an estimate of the allowable spectral bandwidth simply by considering some general aspects of the process.

We start by remarking that for some spatial frequency, $\vec{f}$, and corresponding separation of a pair of points on the aperture, $\lambda\vec{f}$, the mean square turbulence-induced phase difference is

$$D_\phi(\lambda\vec{f}) = 6.88\,(\lambda f/r_o)^{5/3} \tag{39}$$

Here, however, it is more convenient to consider the mean square path length variation for the separation $\vec{L} = \lambda\vec{f}$, which we can write as

$$D_{PL}(\vec{L}) = \left(\frac{\lambda}{2\pi}\right)^2 D_\phi(\vec{L})$$

$$= \frac{6.88}{(2\pi)^2}\left(\frac{L}{r_o\,\lambda^{-6/5}}\right)^{5/3} . \tag{40}$$

Expressed in this form, and recalling the $\lambda^{6/5}$ -dependence of r_o , it is obvious that the turbulence-induced path length variation is wavelength-dependent.

Our requirement determining the allowable spectral bandwidth, $\Delta\lambda$, in forming the speckle photograph (somewhat arbitrarily chosen) is that over the wavelength range λ to $\lambda \pm \frac{1}{2}\Delta\lambda$, the mean square difference of the phase differences associated with a pair of points giving rise to the spatial frequency $\vec{f}$ should be no greater than $(\frac{1}{2}\pi)^2$. It is important to note that while for the wavelength λ , the spatial frequency $\vec{f}$ is associated

https://doi.org/10.1017/S0252921100118639 Published online by Cambridge University Press

with pairs of points on the aperture separated by a distance L , where

$$\vec{L} = \lambda \vec{f} \quad , \tag{41}$$

for the wavelength $\lambda + \frac{1}{2}\Delta\lambda$, this spatial frequency is associated with pairs of aperture points separated by a distance $\vec{L} + \frac{1}{2}\Delta\vec{L}$, where

$$\Delta\vec{L} = \Delta\lambda\, \vec{f} \quad . \tag{42}$$

The difference of path length variations in the one case is $\mathcal{Q}(\vec{r}) - \mathcal{Q}(\vec{r} + \vec{L})$, and the corresponding phase shift is $(2\pi/\lambda)[\mathcal{Q}(\vec{r}) - \mathcal{Q}(\vec{r} + \vec{L})]$, while in the other case the difference of path length variations is $\mathcal{Q}(\vec{r} - \frac{1}{4}\Delta\vec{L}) - \mathcal{Q}(\vec{r}+\vec{L}+\frac{1}{4}\Delta\vec{L})$, and the corresponding phase shift is $[2\pi/(\lambda+\frac{1}{2}\Delta\lambda)][\mathcal{Q}(\vec{r}-\frac{1}{4}\Delta\vec{L}) - \mathcal{Q}(\vec{r}+\frac{1}{4}\Delta\vec{L})]$. The mean square difference of these two phase shifts is

$$\mathfrak{D} = \left\langle \left\{ \left(\frac{2\pi}{\lambda}\right) [\mathcal{Q}(\vec{r}) - \mathcal{Q}(\vec{r}+\vec{L})] - \left(\frac{2\pi}{\lambda+\frac{1}{2}\Delta\lambda}\right) [\mathcal{Q}(\vec{r}-\tfrac{1}{4}\Delta\vec{L}) - \mathcal{Q}(\vec{r}+\vec{L}+\tfrac{1}{4}\Delta\vec{L})] \right\}^2 \right\rangle . \tag{43}$$

After a bit of manipulation, this can be recast in the form

$$\mathfrak{D} = D_\phi(\vec{L}) + \left(\frac{\lambda}{\lambda+\frac{1}{2}\Delta\lambda}\right)^2 D_\phi(\vec{L} + \tfrac{1}{2}\Delta\vec{L})$$

$$- 2\left(\frac{\lambda}{\lambda+\frac{1}{2}\Delta\lambda}\right) D_\phi(\vec{L} + \tfrac{1}{4}\Delta\vec{L}) + 2\left(\frac{\lambda}{\lambda+\frac{1}{2}\Delta\lambda}\right) D_\phi\,(\tfrac{1}{4}\Delta\vec{L}) \quad , \tag{44}$$

where all of the D_ϕ-terms are to be understood as applying for a wavelength λ , but with the two-point separation arguments shown. Making use of Eq. (39) and introducing approximations as appropriate, based on the assumption that $\Delta\lambda << \lambda$, we can obtain from Eq. (44) the result that

$$\mathfrak{D} = 6.88 \left(\frac{\lambda\vec{f}}{r_o}\right)^{5/3} \left[2^{-2/3} \left(\frac{\frac{1}{2}\Delta\lambda}{\lambda}\right)^{5/3} - \frac{7}{18}\left(\frac{\frac{1}{2}\Delta\lambda}{\lambda}\right)^2 \right] \tag{45}$$

Thus the requirement that $\mathfrak{D}$ be less than or equal to $(\frac{1}{2}\pi)^2$, applied at the

https://doi.org/10.1017/S0252921100118639 Published online by Cambridge University Press

upper range of spatial frequencies leads to the requirement on allowable spectral bandwidth that

$$\left(\frac{\Delta\lambda}{\lambda}\right)^{5/3} - 0.48997\left(\frac{\Delta\lambda}{\lambda}\right)^{2} = 1.8074\left(\frac{r_o}{D}\right)^{5/3} \tag{46}$$

For large values of D/r_o , which is normally the case, the $(\Delta\lambda/\lambda)^2$ term is relatively inconsequential, and we can approximate that

$$\frac{\Delta\lambda}{\lambda} \approx 1.4264\,\frac{r_o}{D} \quad . \tag{47}$$

Thus for $D/r_o = 20$, we would get an allowed spectral bandwidth of $\Delta\lambda/\lambda \approx 0.0713$, or for $\lambda = 5500$ Å , $\Delta\lambda \approx 392$ Å .

It should be noted that in developing this result, we have not actually made use of the fact that the aperture is a large diameter circle. Rather, we have only used the fact that the highest spatial frequencies the aperture can pass are of the order of D/λ . As a consequence, Eq. (47) is equally applicable for a Michelson stellar interferometer aperture, except that in this case we would replace D by L , the distance between the two apertures of the interferometer.

With this result in hand for allowable spectral bandwidth, there remain only two more questions of constraint in implementing speckle techniques that we wish to treat here. These concern the allowable field-of-view, i.e., the isoplanatism problem, and the allowable exposure time. We shall treat these in the next two sections.

8. ISOPLANATISM

The term "isoplanatism" was originally used to describe a region in the field-of-view of a lens within which the resolution is essentially constant, i.e., independent of the field-angle. In applying the term to the subject of atmospheric turbulence, we expand the definition to relate to more than

https://doi.org/10.1017/S0252921100118639 Published online by Cambridge University Press

merely resolution as defined by the sharpness of the image of a bar chart, or the size of the image of a point source. In applying the term "isoplanatism" to the subject of atmospheric turbulence, we intend to characterize the equivalence of the wavefront distortion for wavefronts coming from different directions. The key term here is "characterize". According to what our system interest was, we would emphasize different aspects of the wavefront distortion, and accordingly, would arrive at somewhat different detailed definitions of isoplanatism. We shall consider isoplanatism in regard to three system concepts, and comment on the nature of isoplanatism for each. We shall consider 1) short exposure conventional imagery mensuration, 2) adaptive optics, and 3) speckle techniques.

In conventional short exposure imagery, we know that random wavefront tilt effects are suppressed. It is this that enhances the sharpness of a short exposure image as compared to a long exposure image. But for a point source, though the image may be sharp, its exact location, being controlled by the random tilt, is uncertain. For precision mensuration of the separation between two point sources, we take note of the fact that if the two point sources are sufficiently close together, they will be subject to the same random angular tilt, while if they are far enough apart, their tilts will be statistically independent. In the one case, the separation measurement will be uninfluenced by the random tilt, while in the other case, the measured separation will contain a random contribution due to the turbulence-induced tilt. We say that in the first case, the same effective wavefront distortion applied and the two point sources were within an isoplanatism region, while in the latter case, the two sources were not in the same isoplanatic region. We refer to this as angle-of-arrival isoplanatism. It is convenient to measure angle-of-arrival isoplanatism in terms of the mean square variation to be expected in the individual, i.e., single short exposure measurements of the separation of a pair of point sources whose angular separation is $\vec{\vartheta}$.

https://doi.org/10.1017/S0252921100118639 Published online by Cambridge University Press

If $\alpha(\vec{\theta})$ denotes the random variation from frame-to-frame in the component along the direction of, $\vec{\vartheta}$, of the apparent angular position of a point source whose actual position is $\vec{\theta}$, then the mean square separation error is

$$D_\alpha(\vec{\vartheta}) = \langle [\alpha(\vec{\theta}) - \alpha(\vec{\theta} + \vec{\vartheta})]^2 \rangle \quad . \tag{48}$$

It can be shown[19] that

$$D_\alpha(\vec{\vartheta}) = D^{-1/3} \int ds\, C_N^2\, F\,(\vartheta s/D) \quad , \tag{49}$$

where the function, F , can be approximated as

$$F(x) = \frac{5.98}{1 + (0.864/x)^2} \quad . \tag{50}$$

Here D is the aperture diameter of the telescope used to form the short exposure images. It is easy to see that for larger values of ϑ , we get

$$\lim_{\vartheta \to \infty} D_\alpha(\vec{\vartheta}) = D_\alpha(\infty)$$

$$= 5.98\, D^{-1/3} \int ds\, C_N^2 \tag{51}$$

Using the data in Fig. 2, we find that $\int ds\, C_N^2 = 3.57 \times 10^{-12}\ m^{1/3}$ for propagation vertically through the atmosphere, so that

$$D_\alpha(\infty) = 2.13 \times 10^{-11}\, D^{-1/3} \quad . \tag{52}$$

On the other hand, when ϑ is not very large and/or D is assumed to be very large, we can reduce Eq. (49) to the form

$$D_\alpha(\vec{\vartheta}) = 8.01\, D^{-7/3} \int ds\, C_N^2\, s^2\, \vartheta^2 \quad . \tag{53}$$

https://doi.org/10.1017/S0252921100118639 Published online by Cambridge University Press

Noting from the data in Fig. 2, that $\int ds\, C_N^2\, s^2 = 1.31 \times 10^{-5}\ m^{7/3}$, we can rewrite this as

$$D_\alpha(\vec{\vartheta}) = D_\alpha(\infty) \left(\frac{\vartheta}{D/H_{AOA}}\right)^2 \quad , \tag{54}$$

where $H_{AOA} = 2.22 \times 10^3 m$. If we wish, we can consider H_{AOA} to be the turbulence scale height for angle-of-arrival isoplanatism, and D/H_{AOA} as the angle-of-arrival isoplanatic patch size. But these results are directly applicable only for angle of arrival isoplanatism.

For adaptive optics, the isoplanatism conditions are quite different. In this case, instead of being interested in the aperture average wavefront tilt for wavefronts coming from two directions, in the case of adaptive optics, we are interested, on a point by point basis, in how well the wavefront distortion of a reference wavefront matches the distortion of the wavefront to be compensated — a wavefront which is coming from another direction. Actually, our concern is with the matching of the phase difference wavefront against the difference for the wavefront to be compensated.

It has been shown[20] that in this case, the mean square residual phase error after wavefront compensation, and thus the optical transfer function of the adaptive optics system, will be a function of the separation of the pairs of points on the aperture, and thus, of the spatial frequency in the image which we are concerned about. After wavefront distortion compensation by the adaptive optics, the optical transfer function is not quite at its diffraction-limited value, being less than that by a factor of

$$\mathcal{R}_{AO}(\vec{\vartheta}, \vec{f}) = \exp\left[-\mathcal{M}(\vec{\vartheta}, \vec{f})\right] \quad . \tag{55}$$

Here $\vec{\vartheta}$ is the angular separation between the direction of the reference source and the direction of the object whose wavefront is to be corrected for

https://doi.org/10.1017/S0252921100118639 Published online by Cambridge University Press

imaging purposes, and the function $\mathcal{M}$ can be written as

$$\mathcal{M}(\vec{\vartheta},\vec{f}) = 114.7\,\lambda^{-2}\int ds\, C_N^2\,\{(\lambda f)^{5/3} + (\vartheta s)^{5/3} - \tfrac{1}{2}\,[(\lambda f)^2 + 2\,\lambda s\,\vec{\vartheta}\cdot\vec{f} + (\vartheta s)^2]^{5/6} - \tfrac{1}{2}\,[(\lambda f)^2 - 2\,\lambda s\,\vec{\vartheta}\cdot\vec{f} + (\vartheta s)^2]^{5/6}\} \quad . \tag{56}$$

For spatial frequencies, f, very much larger than $\vartheta s/\lambda$, the quantity in the curly brackets can be approximated by $(\vartheta s)^{5/3}$, and we can write

$$\mathcal{M}(\vec{\vartheta},\vec{f}) \approx 114.7\,\lambda^{-2}\,\vartheta^{5/3}\int ds\, C_N^2\, s^{5/3} \quad . \tag{57}$$

Making use of the fact that

$$r_o^{-5/3} = 16.70\,\lambda^{-2}\int ds\, C_N^2 \quad , \tag{58}$$

we can rewrite Eq. (57) as

$$\mathcal{M}(\vec{\vartheta},\vec{f}) = \left(\frac{\vartheta}{r_o/H_{AO}}\right)^{5/3} \quad , \tag{59}$$

where

$$H_{AO} = \left\{6.88\,\frac{\int ds\, C_N^2\, s^{5/3}}{\int ds\, C_N^2}\right\}^{3/5} \quad . \tag{60}$$

From the data in Fig. 2, we find that $\int ds\, C_N^2\, s^{5/3} = 7.28 \times 10^{-7}\ m^2$, and that $\int ds\, C_N^2 = 3.57 \times 10^{-12}\ m^{1/3}$, so that $H_{AO} = 4.88 \times 10^3\ m$. Not only is this scale height about twice as great as for angle-of-arrival isoplanatism, but because r_o is in general much smaller than the aperture diameter, D, the isoplanatic angle $\vartheta_o = r_o/H_{AO}$ is much smaller for adaptive optics than it is for angle-of-arrival short exposure measurements.

https://doi.org/10.1017/S0252921100118639 Published online by Cambridge University Press

In the application of speckle techniques, isoplanatism problems again show up, altering the fringe contrast of the high spatial frequency components of basic interest to us. The problem here, just as in the case of adaptive optics, is that the phase difference across pairs of points in the aperture is not the same for wavefronts from two different directions — only in this case, this results in two different speckle patterns being formed, one for each source's direction. But the key to the proper functioning of the speckle techniques is that the two sources should produce the same random speckle pattern, merely shifted with respect to each other by an amount indicative of the angular separation of the two sources. It can be shown that because of anisoplanatism effects, at high spatial frequencies the speckle pattern amplitude for that spatial frequency component will be <u>different</u> from the value we would expect in the absence of anisoplanatism. This unreliability of the information* can be shown to become significant when $\mathcal{M}(\vec{\vartheta},\vec{f})$, the quantity defined above for the adaptive optics case, gets to be of order unity or greater. Thus the isoplanatism conditions for speckle techniques are basically the same as for adaptive optics.

This result is, in a sense, somewhat surprising, particularly for the Knox-Thompson technique (to which the above conclusion can be shown to apply). For a large object speckle pattern, we would expect to be able to recover valid speckle data at least by masking the pattern so as to process a small region at a time. One might hope that for the Knox-Thomspon technique this would somehow occur automatically. Yet our isoplanatism analysis has given no indication of the potential of the basic Knox-Thompson technique to achieve anything nearly equivalent to what we would expect to

---

* This unreliability effect can not only make a component that should appear strong in fact appear weak, but it can also make a component that should appear weak appear to be strong. Thus, it can make the results obtained from a pair of equal intensity stars appear to be due to a pair of unequal intensity stars.

https://doi.org/10.1017/S0252921100118639 Published online by Cambridge University Press

accomplish by masking so as to reduce the field-of-view and thus get around the isoplanatism problem a bit at a time.

With these results in hand, we now turn to our final subject, the allowable exposure time. This is treated in the next section.

9. TIME DEPENDENCE

The random wavefront distortion introduced by turbulence is a time-varying function. Wavefront distortion samples taken at widely separated times are essentially uncorrelated, while wavefront distortion samples taken at closely spaced times are highly correlated. For adaptive optics to operate successfully, it is obvious that wavefront distortion measurements must be made and wavefront corrections implemented in a time which is short compared to the time in which the wavefront distortion changes significantly. Obviously, the same sort of considerations must apply for speckle techniques in the sense that the exposure time must be brief enough, or else we will be recording the superposition of two uncorrelated speckle patterns. Because the basic analysis of time dependence has been performed for adaptive optics, it will be convenient to discuss the time dependence in adaptive optics first, and then indicate how these results may be applied to selecting an exposure time for recording a speckle pattern.

A particularly compact discussion of the effect of the time dependence of wavefront distortion on adaptive optics system performance has been developed by Greenwood.[21] Starting with the fact that the time dependence of wavefront distortion is due to the wind "transporting" the turbulence pattern through the propagation path, it can be shown that the high temporal frequency end of the power spectrum associated with phase fluctuation at some point on the aperture is given by

$$\lim_{f\to\infty} F_{\phi}(f) = 1.287\,\lambda^{-2} f^{-8/3} \int ds\, C_N^2\, V^{5/3} \quad , \tag{61}$$

https://doi.org/10.1017/S0252921100118639 Published online by Cambridge University Press

where f is the temporal frequency and V is the component of wind velocity perpendicular to the propagation path. The velocity, V, like the refractive-index structure constant, C_N^2, is a function of position, s, along the propagation path.

If the adaptive optics servo system has a closed loop transfer function, $H(f)$, then it can be shown that the residual phase error due to the finite servo bandwidth, (i.e., the portion of the wavefront distortion that is not corrected because the adaptive optics servo lags behind the more rapidly changing aspects of the wavefront distortion), has a mean square value of

$$\sigma_R^2 = \int_0^\infty df \, |1-H(f)|^2 \, F_\phi(f) \quad . \tag{62}$$

Making use of the fact that for a fast enough servo system, the only portion of the phase fluctuation power spectrum, $F_\phi(f)$, that contributes significantly to this integral is well described by Eq. (61), and noting that for most servos the closed loop transfer function, $H(f)$, is nearly equal to unity up to a cut-off frequency, f_c, at which point the transfer function behaves like an R-C electronic filter, (6dB per octave), with its 3dB-point at f_c, i.e., it behaves as $(1 + i\, f/f_c)^{-1}$, it can be shown that

$$\sigma_R^2 = 4.03 \, \lambda^{-2} \, f_c^{-5/3} \int ds \, C_N^2 \, V^{5/3} \quad . \tag{63}$$

Thus the required servo bandwidth, f_c, needed to insure that the rms residual wavefront error is σ_R is

$$f_c = 2.31 \, \lambda^{-6/5} \, \sigma_R^{-6/5} \left\{ \int ds \, C_N^2 \, V^{5/3} \right\}^{3/5} \quad . \tag{64}$$

We infer from typical data on wind speeds aloft[22] that wind speed varies nearly linearly with altitude, and can be approximated by the expression

$$V = 5 + 0.00912 \, h \tag{65}$$

https://doi.org/10.1017/S0252921100118639 Published online by Cambridge University Press

where h denotes altitude, in meters, and the additive value of 5 is introduced to correspond to a nominal low level wind velocity. Using the data in Fig. 2, we can approximate

$$\int ds\, C_N^2\, V^{5/3} \approx 3.42 \times 10^{-10}\ m^2\text{-sec}^{-5/3} \quad , \tag{66}$$

so that

$$f_c \approx 4.83 \times 10^{-6}\, \lambda^{-6/5}\, \sigma_R^{-6/5}$$

$$= 157 \left(\frac{0.55 \times 10^{-6}}{\lambda}\right)^{6/5} \sigma_R^{-6/5} \quad . \tag{67}$$

If we wished the adaptive optics servo to provide an rms residual wavefront error of a twentieth of a wave, i.e., $\sigma_R = \pi/10$, then the required servo bandwidth for operation at $\lambda = 0.55 \times 10^{-6}$ m would be $f_c = 630$ Hz .

The same general approach can be applied to the problem of defining an allowable exposure time for the recording of a speckle pattern. In this case, our concern is with the rms change in the wavefront pattern during the exposure. This change is associated with the high temporal frequency portion of the wavefront variations, with the meaning of high temporal frequency being defined by the exposure time. If the shutter opens sharply, remains open for a time T , and then closes sharply, it may be considered to "pass" temporal frequencies in accordance with the transfer function

$$H(f;T) = \frac{\sin(\pi f T)}{\pi f T} \quad . \tag{68}$$

In the higher frequency range, i.e., $f > T^{-1}$, the fluctuations will be averaged over a significant range of variations, while at the lower frequencies the variation will "stand still" during the exposure time.

https://doi.org/10.1017/S0252921100118639 Published online by Cambridge University Press

It is clear that we can apply Eq. (62), with the transfer function as defined by Eq. (68), to determine the mean square phase variation during an exposure. Thus we can write

$$\sigma_E^2 = \int_0^\infty df \left| 1 - \frac{\sin(\pi f T)}{\pi f T} \right|^2 1.287 \lambda^{-2} f^{-8/3} \int ds\, C_N^2\, V^{5/3} . \quad (69)$$

Noting that

$$\int_0^\infty dx\, x^{-8/3} \left| 1 - \frac{\sin(\pi x)}{\pi x} \right|^2 = 1.416 \quad (70)$$

and making use of Eq. (66), we obtain the result that

$$\sigma_E^2 = 6.23 \times 10^{-10} \lambda^{-2} T^{5/3}$$

$$= 2.06 \times 10^3 \left(\frac{0.55 \times 10^{-6}}{\lambda} \right)^2 T^{5/3} . \quad (71)$$

It thus follows that if we are prepared to allow a wavefront distortion variation of σ_E during each short exposure, the exposure time, T, must be

$$T = 0.0103 \left(\frac{\lambda}{0.55 \times 10^{-6}} \right)^{6/5} \sigma_E^{6/5} \text{ sec} . \quad (72)$$

Thus if we will allow a phase shift of $\frac{1}{2}\pi$ during the exposure, working at a wavelength of $\lambda = 0.55 \times 10^{-6}$ m, the allowable exposure time is 17.6 msec.

It should be noted here that we may have been overly generous in allowing an rms phase variation of $\frac{1}{2}\pi$, and allowing the same phase variation with wavelength in selecting the allowable bandwidth for speckle techniques. The formulas we have presented will allow evaluation of the useful spectral bandwidth and the allowable exposure time for other estimates of what is a tolerable phase variation. It is unfortunate, however, that the

https://doi.org/10.1017/S0252921100118639 Published online by Cambridge University Press

necessary theory does not exist to permit us to relate the spectral bandwidth and exposure time to the optical transfer function directly and quantitatively — and thus we are forced to use a plausible value for the allowable phase error. Nonetheless, the formulas presented here do provide a reasonably sound basis for estimation of spectral bandwidth and exposure time.

https://doi.org/10.1017/S0252921100118639 Published online by Cambridge University Press

References

1. A. Kolmogorov, Compt. Rend. (Doklady) de l'Academie des sciences de l'U.S.S.R. 31 , 538 (1941); translated in Turbulence — Classic Papers on Statistical Theory , S. K. Friedlander and L. Topper, Eds. (Interscience Publishers, Inc., New York, 1961)

2. V. I. Tatarski, Wave Propagation in a Turbulent Medium (McGraw-Hill Book Co. Inc., New York, 1961)

3. S. Pond, S. D. Smith, P. F. Hamblin, and R. W. Burling, "Spectrum of Velocity and Temperature Fluctuations in the Atmospheric Boundary Layer Over the Sea", J. Atmos. Sci 23 , 376 (1966)

4. Ting-i Wang, G. R. Ochs, and S. F. Clifford, "A Saturation-Resistant Optical Scintillometer to Measure C_N^2", J. Opt. Soc. Am. 68 , 334 (1978)

5. D. Greenwood, private communication

6. G. E. Mevers, M. P. Keister, Jr., and D. L. Fried, Optical Propagation Measurements at Emerson Lake - 1968 , NASA Contractor Report, NASA CR-1733 , Sept 1971

7. R. L. Kurtz and J. L. Hayes, Experimental Measurements of Optical Angular Deviation Caused by Atmospheric Turbulence and Refraction , NASA Technical Note, NASA TN D-3439, May 1966

8. D. L. Fried, "Propagation of a Spherical Wave in a Turbulent Medium", J. Opt. Soc. Am. 57 , 175 (1967)

9. R. F. Lutomirski, R. E. Huschke, W. C. Meecham, and H. T. Yura, Degradation of Laser Systems by Atmospheric Turbulence , Rand Co. Rpt., R-1171-ARPA/RC, June 1976

10. D. L. Fried, "Optical Heterodyne Detection of an Atmospherically Distorted Signal Wave Front", Proc. IEEE 55 , 57 (1967) — cf also Ref. 15.

11. D. L. Fried and G. E. Mevers, "Evaluation of r_o for Propagation Down Through the Atmosphere", Appl. Opt. 13 , 2620 (1974) ; 14 , 2567 (1975) ; 16 , 549 (1977)

https://doi.org/10.1017/S0252921100118639 Published online by Cambridge University Press

12. D. L. Fried, "Statistics of a Geometric Representation of Wavefront Distortion", J. Opt. Soc. Am. 55 , 1427 (1965).

13. R. J. Noll, "Zernike Polynomials and Atmospheric Turbulence", J. Opt. Soc. Am. 66 , 207 (1976).

14. R. E. Hufnagel and N. R. Stanley, "Modulation Transfer Function Associated with Image Transmission Through Turbulent Media", J. Opt. Soc. Am. 54 , 52 (1964).

15. D. L. Fried, "Optical Resolution Through a Randomly Inhomogeneous Medium for Very Long and Very Short Exposures", J. Opt. Soc. Am. 56 , 1372 (1966).

16. A. Labeyrie, "High-Resolution Techniques in Optical Astronomy", in Progress in Optics Vol. XIV , E. Wolf Ed., (North Holland Publishing Co., Amsterdam, 1976).

17. K. T. Knox and B. J. Thompson, "Recovery of Images from Atmospherically Degraded Short-Exposure Photographs", Ap. J. 193 , L45 (1974).

18. D. Korff, "Analysis of a Method for Obtaining Near-Diffraction-Limited Information in the Presence of Atmospheric Turbulence", J. Opt. Soc. Am. 63 , 971 (1973).

19. D. L. Fried, "Angle-of-Arrival Isoplanatism", Part II of Theortical Study of Non-Standard Imaging Concepts , Rome Air Development Center Rpt No. RADC-TR-76-51, March 1976.

20. D. L. Fried, "Isoplanatic Aspects of Predetection Compensation Imagery", Chap I of Theoretical Study of Non-Standard Imaging Concepts, Rome Air Development Center Rpt. No. RADC-TR-74-185.

21. D. P. Greenwood, "Bandwidth Specification for Adaptive Optics Systems", J. Opt. Soc. Am. 67 , 390 (1977).

22. I. I. Gringorten, R. W. Lenhand, Jr., H. A. Salmela, and N. Sissinwine, "Winds" Fig. 4 - 23, in Handbook of Geophysics and Space Environments , S. L. Valley, Ed. (McGraw-Hill Book Co.,Inc., New York, 1965).

https://doi.org/10.1017/S0252921100118639 Published online by Cambridge University Press

DISCUSSION

J.C. Dainty: Whilst I agree that the classical resolution is not affected by non-isoplanicity (in speckle interferometry), the signal to noise ratio of a measurement is reduced.

D.L. Fried: Certainly.

R.Q. Twiss: Michelson never saw the secondary maxima of $|\Gamma|^2$ in his interferometric measurements of the Galilean satellites. Is it not possible that this was due, in large part, to the fact that the angular sizes of the satellites were greater than the isoplanatic patch?

D.L. Fried: While we are not certain of the exact size of the isoplanatic angle θ_o, it is probable that, although the satellite angular diameters are smaller than θ_o, they are comparable to it, so that there would be some (mild) anisoplanatism effects. Extrapolating from my results for a pair of point sources to a disk source, I would estimate that anisoplanatism would result in spurious limb darkening of the disk. This could account for Michelson's failure to observe secondary maxima.

https://doi.org/10.1017/S0252921100118639 Published online by Cambridge University Press